SYSTEM THEORY, CONTROL AND COMPUTING JOURNAL

Vol. 1, No. 1, June 2021

ISSN 2668-2966

Editura UNIVERSITARIA
Craiova, 2021

CONTACT
SYSTEM THEORY, CONTROL AND COMPUTING JOURNAL
University of Craiova, No. 13, A.I. Cuza Street, Craiova, 200585, Dolj, Romania
Phone: 0251 438 198
Email: stcc.journal@ucv.ro
Website: http://stccj.ucv.ro/

ISSN 2668-2966
ISSN-L 2668-2966

Editorial Team

Editors and Publisher

Editors
Faculty of Automation, Computers and Electronics of The University of Craiova, Romania
Faculty of Automation and Computers of The Politehnica University of Timișoara, Romania
Faculty of Control Systems, Computers, Electrical and Electronics Engineering of The "Dunărea de Jos" University of Galați, Romania
Faculty of Automatic Control and Computer Engineering of The "Gheorghe Asachi" Technical University of Iași, Romania

Publisher
Editura Universitaria, Str. A.I. Cuza, 13, 200585 Craiova, Romania
https://www.editurauniversitaria.ro/ro

Editorial Board

FOREWORD

In front of the reader – a new scientific journal: The *System Theory, Control and Computing Journal*. It is not quite new since it occurred from merging of 4 journals traditionally (along some half-century) edited by Control and Computing Engineering departments and faculties (schools) from the University of Craiova, Technical „Gheorghe Asachi" University of Iaşi, „Dunărea de Jos" University of Galaţi and Politehnica University of Timişoara. Continuing these journals in a merged and improved form, it aims promoting theoretical and applied results in a large field of System Theory, Control and Computing (with particular reference to Applied Informatics and Applications in Systems and Control). From expression of the academic life in the aforementioned departments, this journal aims to become a more comprehensive publication, integrating the research results of a broad scientific and technical community. The access to publication of research results is open to researchers all over the world.

This starting issue of the new journal is a good illustration of the editorial intentions, assertion proven by a short glance at the 11 firstly published papers.
Ranging from *genuine Systems and Control Theory* (σ-entropy in stochastic linear systems, nonlinear observability of polynomial dynamical systems or steady state motion control for mechanical systems), to *Applied Control* (nonlinear MPC for hydrostatic transmissions, Kalman filter design for distributed parameter systems in biotechnology, backward path tracking control for trailer systems), *intelligent control based instrumentation* (baseline removal in Gamma Spectroscopy, state estimation for sensor networks with low computer capabilities), *applied informatics* (logistic stability examination in serial and arborescent topologies) up to *computer applications and software development* (automatic control knowledge repository and automatic generation of object oriented code), the first issue of the new journal is a genuine promising of broadband covering scientific and engineering interests.

The Editorial Board

SYSTEM THEORY, CONTROL AND COMPUTING JOURNAL, VOL. 1, NO. 1, JUNE 2021, pp. 1-12

Baseline Removal in Spectrometry Gamma by Observation of Local Minima

Kélian This
Commissariat à l'énergie atomique (CEA)
Nuclear measurement laboratory
21120, Valduc, France
kelian.this@cea.fr

Laurent Le Brusquet
Université Paris-Saclay, CNRS, CentraleSupélec
Laboratoire des signaux et systèmes
91190, Gif-sur-Yvette, France

Adrien Frigerio
Commissariat à l'énergie atomique (CEA)
Nuclear measurement laboratory
21120, Valduc, France

Sébastien Colas
Commissariat à l'énergie atomique (CEA)
Nuclear measurement laboratory
21120, Valduc, France

Pascal Bondon
Université Paris-Saclay, CNRS, CentraleSupélec
Laboratoire des signaux et systèmes
91190, Gif-sur-Yvette, France

***Abstract*—This paper presents a Baseline Removal method in the context of spectrometry gamma. The method implements an estimator for the full continuum based on the observation of local minima. This estimator is constructed from the statistical properties of the signal and is therefore easily explainable. The method involves a limited number of fixed parameters, which allows the automation of the process. Moreover, the method is adaptable to any peaks width, which makes it suitable for both HPGe spectrometers and scintillators. Application to real gamma spectrometry measurements are presented, as well as a discussion about the choice of the parameters, for which an adjustment is proposed.**

***Index Terms*—background removal, baseline correction, gamma spectrometry, continuum estimation, peak characterization, local minima**

I. Introduction

A. Context

Gamma spectrometry is a common nuclear measurement technique which can be used for the detection of radioactivity, identification of radionuclides, and quantification of radioactive material. Eventhough other methods exist, in practice, the gamma spectrometry often constitutes the only possible and effective technique, especially for waste characterization [1]. As a consequence, gamma spectrometry has become essential in the nuclear sector.

One will find in [2] a complete description of gamma rays Physics as well as a number of details relating to the measurement device. The result of a measurement is a histogram, called spectrum, which spreads detected photons by channels each corresponding to an interval of energy. All spectra have the same structure, that is to say a superposition of a background with peaks specific to some radionuclides, covered by an observation noise. Peaks are mathematically described by a mixture model, usually Gaussian [2, section 9.6] [3, p.229] but not only [4], which contains a great deal of useful information. On the opposite, the background, also called continuum which is rather regular and smooth contains few information (at least, with regard to the peaks).

The purpose of the spectrum analysis is to estimate the mixture parameters from the data. Consequently, continuum is of little interest and one of the major issue of the spectrum analysis is to isolate the mixture from the continuum. Baseline Removal (BR) methods enable to estimate the continuum without any consideration for the peak mixture, then to subtract it from the spectra in order to isolate the peak mixture. This technique can also be found in Literature under the appellation "background correction", or a mix of both expressions. However, "baseline" is less ambiguous than "background" which may also refers to the radiation from the environment. Moreover, "removal" is more appropriate that "correction" because it would implies the continuum to be an error, which is not the case.

B. State of the Art

BR techniques is is a recurrent topic in gamma spectrometry, but also in other spectroscopy issues [5]. From the very beginning in the 70s to nowadays, two distinct strategies have been brought to light: local and global.

Local Baseline Removal (LBR) methods enable to estimate derive a local estimate of the continuum on a given Region Of Interest (ROI) of the spectrum, i.e. in the vicinity of a peak, by the observation of points of the pure continuum at the outer left and right borders of the ROI

Cite as: K. This, L. Le Brusquet, A. Frigerio, S. Colas, and P. Bondon, "Baseline removal in spectrometry gamma by observation of local minima", *Syst. Theor. Control Comput. J.* , vol. 1, no. 1, pp. 1–12, Jun. 2021.
DOI: 10.52846/stccj.2021.1.1.4

[6] [7] [8] [9] [2, sections 5.4]. LBR requires to established the ROI beforehand by the use of a Peak Detection (PD) method.

Full Baseline Removal (FBR) methods estimate the whole continuum of the spectrum, without introducing the concept of ROI, and does not rely on a PD method. Among FBR techniques, one finds filtering [10], peak erosion [11] [12] [13] [3, p.256] [14], penalizing or regularization criterion [15] [16] [17] [18] [19] [20] [21] [22] [23], and observation of local minima [24] [25] [26] [27] [28] [29].

Nowadays, those propositions were naturally ranked by the operating experience, and LBR [2, sections 5.4] coupled to the PD second derivative method [30] is commonly used and officially recommended [31] [32]. This method chiefly draws its success from its simplicity and explainability. However, it remains difficult to be automated and may fail in the presence of Compton edges or multiplets, i.e. mixtures of close overlapping peaks. On the other hand, a large number of proposed global methods involve a model for the continuum (splines, Gaussian processes etc), which introduce an improper regularity prior: continuum often contains discontinuities which are difficult to model. Thus, spectrum analysis is still an active research topic.

C. Content

Beyond the performance criterion, an ideal method should enables the automation of the analysis with a large scope of application. It shall deal with various peaks shapes and widths, with various radiation detectors technologies, i.e. Hyper Pure Germanium (HPGe) detectors as well as scintillators. The method shall admit a reduced set of parameters independent from the observation.

The central idea of the present study relies on the following empirical observation: local minima rarely appear on peaks. Thus, it would be possible to estimate the continuum from local minima. As mentioned in the state of the Art, several authors have approached this idea, but the work of Tervo et al. [27] is the most accomplished: it enables to simplify the estimation of the continuum without any prior nor any parameters. However, this estimator only works with thin peaks which quickly limits its use for real applications.

This paper takes up, corrects and extends previous developments [33]. This work presents a BR method adapted to gamma spectrometry also based on the observation of local minima. Fig. 1 presents the application of the method of Tervo and of the new method on two representative spectra. The improvement is easily noticeable on the figure, and shows that the new method covers a much wider range of spectra configurations (the comparison will be detailed in part IV). The resulting process is simple to apply. The paper is focused on the statistical phenomenon which enables the method to give good results.

Section II, on one hand, gives a definition of the spectrum. On the other hand, it deducts a number of inherent signal properties on which is built the continuum estimation procedure in section III. Section IV comments the real spectra application, and section V concludes this work.

II. Spectrum signal properties

This section aims at formalizing the problem and proposes some general properties about a gamma spectrum and its components.

A. Basic assumptions

Let $\boldsymbol{y}$ denote the observed gamma spectrum of n channels such that $\boldsymbol{y} = (y_1, \dots, y_n)$. Let $\boldsymbol{m} = (m_1, \dots, m_n)$ denote the peaks mixture and $\boldsymbol{c} = (c_1, \dots, c_n)$ the continuum. Denoting $\mathcal{P}$ the Poisson's distribution, Physics states [2, section 5.2] $\boldsymbol{y}$ is a sample from a random vector $\boldsymbol{Y} = (Y_1, \dots, Y_n)$ such that:

$$Y_k \sim \mathcal{P}(\mu_k) \tag{1}$$

where $\boldsymbol{\mu} = \boldsymbol{m} + \boldsymbol{c}$ is the noiseless signal.

Poisson distribution is not practical to handle in literal calculations. Denoting $\mathcal{N}$ the normal distribution and assuming that the spectrum has a sufficient number of count per channel, the following approximation is possible [34, section 2.7.3]:

$$\mathcal{P}(\mu_k) \approx \mathcal{N}(\mu_k, \mu_k) \tag{2}$$

By the properties of the Poisson distribution [34, section 13.5.5], y_k is itself an estimate for μ_k and the associated confidence interval with symmetric risks of level $1-\eta$ is:

$$\frac{1}{2}\chi^2_{2y_k;\eta/2} \leq \mu_k \leq \frac{1}{2}\chi^2_{2(y_k+1);1-\eta/2} \tag{3}$$

where $\chi^2_{v;\eta}$ is the quantile of order η of a χ^2 distribution with v degrees of freedom. Using this property in order to quantify the variance of the observation, one may assume the following hypothesis:

Hypothesis 1:

$$\left\{ \begin{array}{lcl} Y_k & \sim & \mathcal{N}(\mu_k, \sigma_k^2) \\ \sigma_k^2 & = & y_k \end{array} \right. \tag{4}$$

The issue can now be specified: knowing $\boldsymbol{y}$, how to estimate $\boldsymbol{c}$? Because $\boldsymbol{m}$ is also unknown, the problem is unsolvable at this stage: a prior is required. In the paragraphs below, one is looking for a discrimination criterion, through the definitions of peaks and continuum, which may be used as the missing constraint.

B. Signal characterization

Let introduce the differential operator $\Delta x_k = x_k - x_{k-1}$. The continuum is characterized by its low variations. Thus, continuum variations are majorated:

$$\exists \beta, \quad \forall k, \quad |\Delta c_k| \leq \beta \tag{5}$$

A peak has characteristic areas. A top, at the center, has high values and low variations. Two flanks, uprising and downrising on both sides of the top, have high variations, especially in comparison with continuum variations. Two

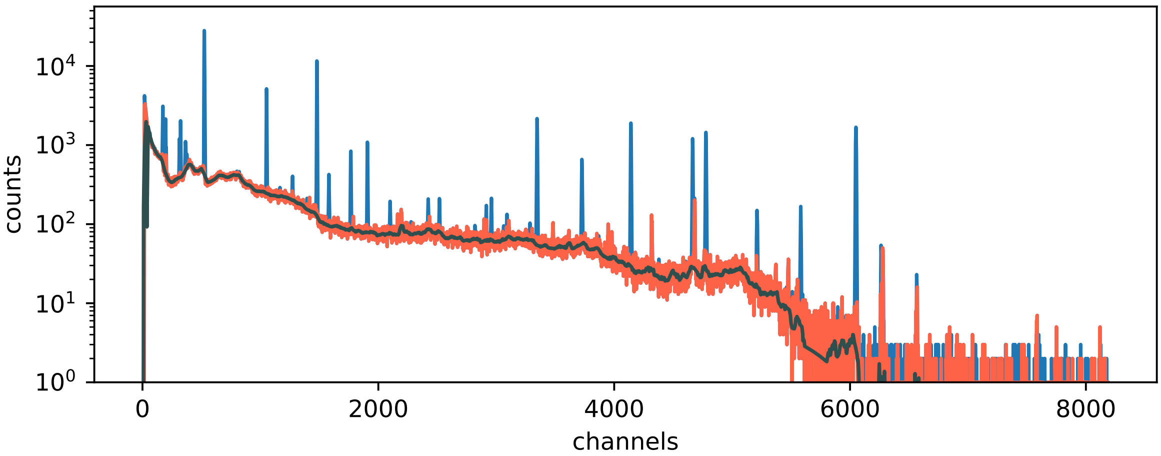

(a) HPGe

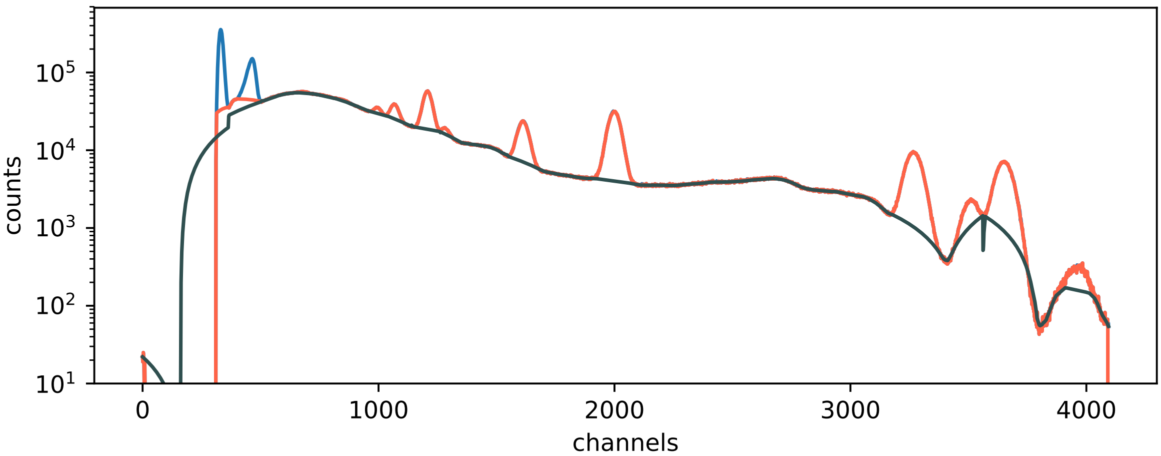

(b) Scintillator

Fig. 1: Confrontation of continuum estimation methods on real spectra. On top is a HPGe spectrum, on the bottom a scintillator spectrum. Both are plotted with a log scale. Blue lines represent the observation. Orange lines represent the reference estimates of Tervo's method. Black lines represent the new method results, applied with parameters $t_{\text{break}} = 3$, $w_{\text{opt}} = 15$, $w_f = 11$, $o_f = 1$ and $w = 6$ for HPGe, $w = 80$ for scintillator.

flats at the borders have low values and low variations. Let denote $\mathbb{F}$ the set of all flanks in the spectrum. Then, $\overline{\mathbb{F}}$ contains all tops and flats. The borders of the areas are thereby defined by means of a threshold α such that:

$$\beta \leq \alpha, \quad \forall k \in \mathbb{F}, \quad \alpha \leq |\Delta m_k| \tag{6}$$

The unfixed threshold α is a necessary scaling variable, and its choice is a matter of convention. Indeed, what could be considered as a peak in a certain context could be considered as a continuum contribution in another. Fig. 2 shows a mono peak signal with a constant continuum. Choosing $\alpha = 50$, resulting $\mathbb{F}$ areas are represented with grey bands.

As a consequence of the previous definitions, one can deducts a lower bound for the variations of the signal:

Property 1:

$$\forall k \in \mathbb{F}, \quad \alpha - \beta \leq |\Delta \mu_k| \tag{7}$$

C. Counter variations

Let denote respectively $\mathbb{F}^+$ and $\mathbb{F}^-$ the set of increasing flanks and the set of decreasing flanks:

$$\begin{cases} \mathbb{F}^+ &= \{k \in \mathbb{F} | \alpha \leq \Delta m_k\} \\ \mathbb{F}^- &= \{k \in \mathbb{F} | \Delta m_k \leq -\alpha\} \end{cases} \tag{8}$$

$\forall k \in \mathbb{F}$ let F_k be the probability to have a counter-variation in $\boldsymbol{y}$ at k. More specifically, F_k is the probability

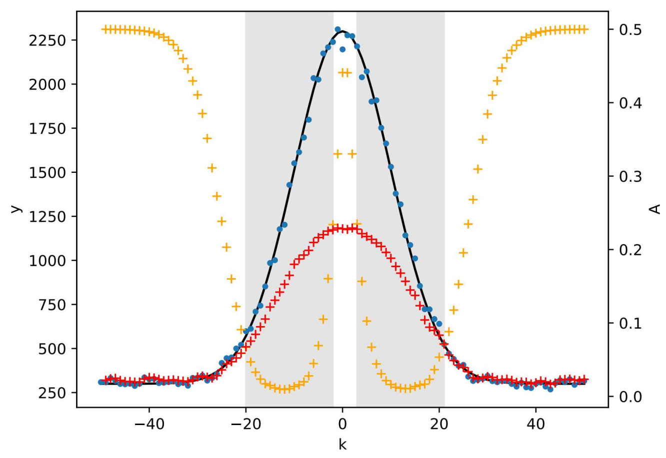

Fig. 2: Identification of peak's areas on a Gaussian example. Dark full line represents the signal $\boldsymbol{\mu}$, blue points represent observations $\boldsymbol{y}$, grey bands indicates $\mathbb{F}$, orange crosses represent $\boldsymbol{A^{lim}}$, red crosses represent $\boldsymbol{A}$.

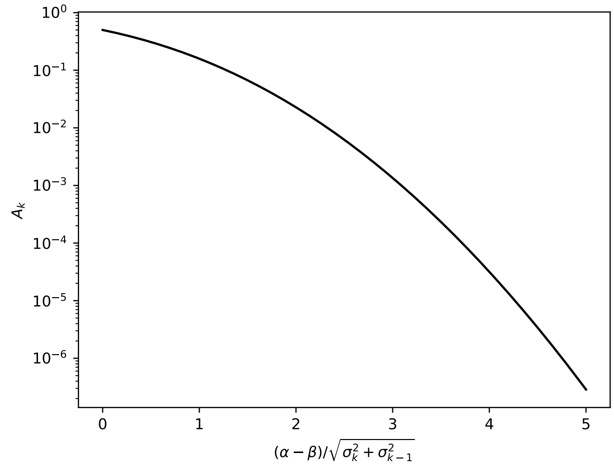

Fig. 3: A_k values on a log scale.

for $\boldsymbol{y}$ to decrease where $\boldsymbol{m}$ is increasing, or to increase where $\boldsymbol{m}$ is decreasing:

$$F_k = P(\Delta Y_k \leq 0 | k \in \mathbb{F}^+) \tag{9}$$
$$= P(0 \leq \Delta Y_k | k \in \mathbb{F}^-) \tag{10}$$

Notice that F_k is almost the repartition function of $\Delta Y_k \sim \mathcal{N}(\Delta\mu_k, \sigma_k^2 + \sigma_{k-1}^2)$ evaluated at 0. Let denote $\Phi(.)$ the cumulative distribution function (CDF) of the standard normal distribution. Thanks to property 1 and noticing Φ is an increasing function, one has an upper bound for F_k:

Property 2:

$$\forall k \in \mathbb{F}, \quad F_k \leq A_k = \Phi\left(\frac{-(\alpha-\beta)}{\sqrt{\sigma_k^2 + \sigma_{k-1}^2}}\right) \tag{11}$$

On Fig. 2 is plotted $\boldsymbol{A} = (A_1, ..., A_n)$ for $\alpha = 50$ and $\beta = 0$. Because this signal is a simulation, one exactly knows the value of Δm_k, which allows to evaluate the admissible limit values for $\boldsymbol{A}$ as follows:

$$A_k^{lim} = \Phi\left(\frac{-\Delta m_k}{\sqrt{\sigma_k^2 + \sigma_{k-1}^2}}\right) \tag{12}$$

One notes through $\boldsymbol{A^{lim}} = (A_1^{lim}, ..., A_n^{lim})$ that counter-variations probabilities are close to zero on high variations areas. This observation is confirmed by Fig. 3 where the value of A_k quickly decreases.

D. Focus on local minima

Let introduce ξ, the set of indexes of $\boldsymbol{y}$ local minima:

$$\xi = \{k | y_k < y_{k-1}, y_k < y_{k+1}\} \tag{13}$$

1) Local minima bias: As shown in Fig. 4, the local minima set is biased because local minima's expectation is not equal to the signal expectation. Moreover, the figure shows that local minima are less dispersed than the observation. It makes sense because local minima are less likely to have a value above μ. Let $\varphi(.)$ denote the probability density function (PDF) of the standard normal distribution.

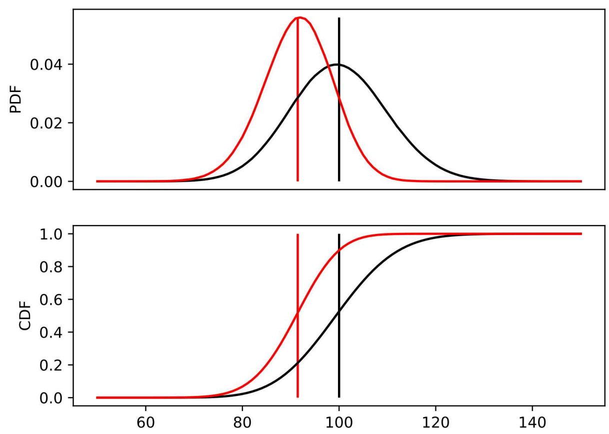

Fig. 4: Local minima's expectation bias for $\mu = 100$. Black is associated with the full signal, red is associated with its local minima. Vertical lines indicate expectations of the distributions.

Property 3: One has:

$$\begin{cases} \mathrm{E}(y_{\xi_i}) & = & \mu_{\xi_i} + \sigma_{\xi_i}\dfrac{C_1}{C_0} \\ \mathrm{V}(y_{\xi_i}) & = & \sigma_{\xi_i}^2\left(\dfrac{C_2}{C_0} - \left(\dfrac{C_1}{C_0}\right)^2\right) \end{cases} \tag{14}$$

where

$$C_i = \int_{-\infty}^{+\infty} u^i \varphi(u)(1-\Phi(u))^2 du \tag{15}$$

Note that C_0 is the density of ξ for a stationary signal. Numerical integration results in the following values:

$$\begin{cases} C_0 = & 1/3 \\ C_1 \approx & -0.28209479 \\ C_2 \approx & 0.42522148 \end{cases} \tag{16}$$

The reduction of the variance of the local minima that one noticed on Fig. 4 may now be quantified:

$$\frac{\mathrm{V}(y_{\xi_i})}{\sigma^2_{\xi_i}} = \frac{C_2}{C_0} - \left(\frac{C_1}{C_0}\right)^2 \approx 0.55946721 \tag{17}$$

Property 3 allows one to propose a bias correction:

Property 4: $\hat{\mu}_{\xi_i}$ is an unbiaised estimator of μ_{ξ_i} such that:

$$\begin{cases} \hat{\mu}_{\xi_i} & = & y_{\xi_i} - \sigma_{\xi_i}\dfrac{C_1}{C_0} \\ \mathrm{V}(\hat{\mu}_{\xi_i}) & = & \mathrm{V}(y_{\xi_i}) \end{cases} \tag{18}$$

Proof of properties 3 and 4 is given in the appendix.

2) Occurrence of local minima: One have reported on the Fig. 5 the evaluation by simulation of the probability P_{min} that a point of a linear signal, with a slope γ and a gaussian noise with a standard deviation level σ, is a local minima. Note that $P_{min}(\gamma/\sigma = 0) = C_0$, and P_{min} quickly decreases.

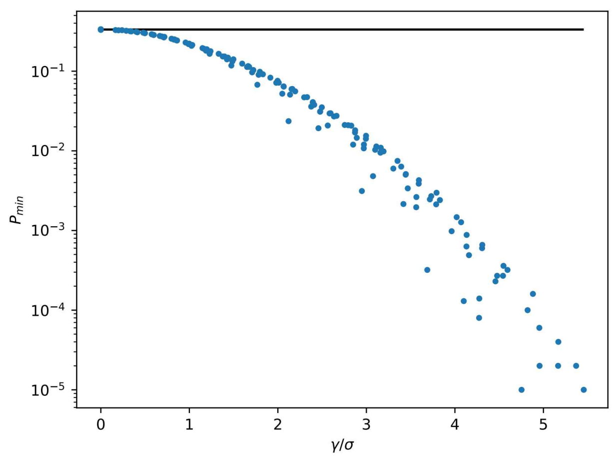

Fig. 5: Blue points represent $P_{min}(\gamma/\sigma)$ on a grid of 20 values of γ linearly spaced on $[0, 100]$ and 20 values of σ spaced evenly on a log scale on $[1, 1000]$. Black line represents C_0.

Additionally, one can deduct from property 2 an upper bound on the probability that a local minima belongs to $\mathbb{F}$:

Property 5:

$$P(k \in \mathbb{F} | k \in \xi) \leq \frac{A_k}{P(k \in \xi)} \tag{19}$$

Proof of property 5 is given in the appendix. One notices that $P(k \in \xi)$ can not be too small, because in practice there is always a non negligible portion of local minima in a measurement. Moreover, Fig. 5 testifies that $\forall k \in \mathbb{F}$, A_k is dramatically low. Therefore, $P(k \in \mathbb{F} | k \in \xi)$ is majorated by a constant close to zero, which explains a remarkable phenomenon easily noticeable through data: local minima are absent from the flanks. It is thus possible to identify points in $\overline{\mathbb{F}}$ by observing ξ:

Hypothesis 2:

$$\xi \subset \overline{\mathbb{F}} \tag{20}$$

Since local minima are easily observable in a given spectrum, hypothesis 2 is a convenient criterion upon which one may build an estimator for the continuum.

III. Continuum estimation

A. Intruders filtering

In the previous section, one identified points from $\overline{\mathbb{F}}$. However, this is not exactly what one was looking for (we are looking for $\boldsymbol{c}$ where $\boldsymbol{m}$ is omitted). Some undesirable intruders are present in ξ, as shown in Fig. 6. Indeed, it contains top points which must be removed. Moreover, local minima may accidentally appear on the flank of a significant peak. In any case, all intruders values are substantially higher than those of the points attached to the continuum. This gives us an opportunity to filter them. One assumes y_{ξ_i} is a sample from a random variable $Y_i^{\min}$ such that:

Hypothesis 3:

$$Y_i^{\min} \sim \mathcal{N}(\mathrm{E}(y_{\xi_i}), \mathrm{V}(y_{\xi_i})) \tag{21}$$

Note that Hyp. 3 is actually an approximation of the true distribution of the local minima, but which simplifies the definition of the process of discontinuity detection.

Let define the null hypothesis $H0$:≪ there is no discontinuity between ξ_{i-1} and ξ_i ≫. Let t_{break} be the $1-\eta/2$ order quantile of $\mathcal{N}(0,1)$ and:

$$z_i = \frac{|\Delta y_{\xi_i}|}{\sqrt{\mathrm{V}(y_{\xi_i}) + \mathrm{V}(y_{\xi_{i-1}})}} \tag{22}$$

By Hyp. 3, the variable z_i is a z-score for $H0$. Consequently, if $t_{\text{break}} \leq z_i$, one can reject $H0$ with a confidence η.

By selecting a threshold t_{break} for this hypothesis testing, one detects discontinuities in ξ, and forms groups of continuous ξ sets. Then one observes the sign of Δy_{ξ_i} at the groups borders. This reveals groups which levels are higher than those of their direct neighbours. These are intruders groups to be filtered as shown on Fig. 6.

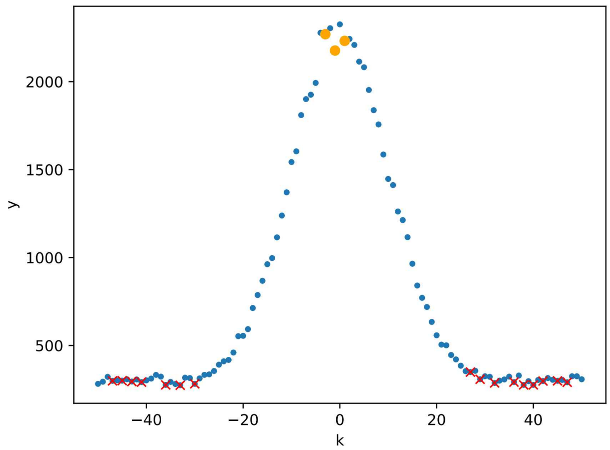

Fig. 6: Intruders filtering with $t_{\text{break}} = 1.5$. Blue points represent observations $\boldsymbol{y}$, red crosses represent remaining ξ after intruders filtering, orange points represent intruders.

B. Large peaks issue

Previous intruders filtering is able to deal with GeHP thin peaks spectra. But when facing peaks acquired by a scintillator, peaks are very large with respect to $\mathbb{F}$ variations, and the estimator fails as shown on the top plot in Fig. 7. A simple solution is to subsample the signal before filtering the intruders as shown on the middle plot in Fig. 7. This means that from the relevant spectrum, one keep one point out of p, starting at point s. Parameter p is the subsampling step, s the subsampling offset such as $0 \leq s < p$. In this manner, the variation rate between two points is multiplied by p, whereas the noise level has not changed, which allows to fix the large peaks issue.

To limit the information loss due to subsampling, one selections subsamples of ξ successively with all possible values of s for a given p in order to produce p subsets of points of the continuum. Then subsets are merged as illustrated on the bottom plot in Fig. 7.

Actually, when facing large peaks, subsampling is a trick which allows to fall back on a thin peaks analysis issue. An optimum choice for p depends on (i) w, the actual full width at half maximum (FWHM) of the peaks and on (ii) w_{opt}, a fix ideal FWHM that one strives to retrieve. This offers a meaningful alternative parametrization for the estimator:

$$p = \max\left(1, \lfloor \frac{w}{w_{\text{opt}}} \rfloor\right) \tag{23}$$

C. Noise filtering and interpolation

In previous developments, one found points ξ in the signal where peak levels are negligible. However, the continuum has yet to be dissociated from the observation noise by a filtering operation. Furthermore, one has to fill

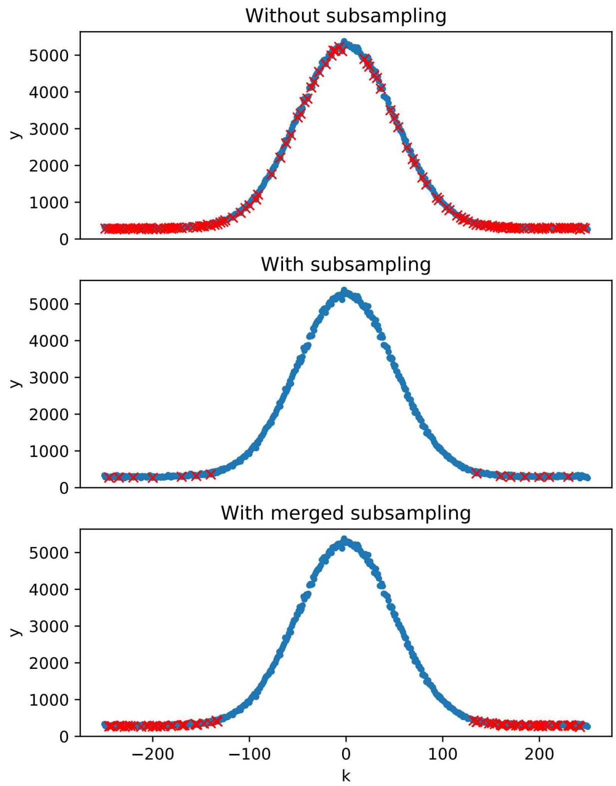

Fig. 7: Subsampling effect on outlier filtering with $t_{\text{break}} = 1.5$. Top figure uses no subsamplings, middle figure uses subsampling ($p = 5$, $s = 0$), bottom figure uses merged subsamplings ($p = 5$). Blue line represents observations $\boldsymbol{y}$, red crosses represent remaining ξ after intruders filtering.

missing values at channels which does not present local minima.

Every filter is built on a regularity prior for the clean signal that one strives to retrieve. The smoothness of the continuum suggests it can locally be described by a polynomial expression. If continuum presents some discontinuities which undermines the polynomial assumption, these are difficult to take into consideration because of our ignorance of the continuum and one merely assumes this event is rare and sets it aside.

The proposed filtering process at ξ_i then consists in the fit of a polynom of order o_f on a odd window of w_f contiguous points of ξ centered in ξ_i. This filter is similar to a Savitzky-Golay filter [35] but with a nonuniform sampling step as points of ξ are not evenly spaced. In a second time, a linear interpolation fills the missing parts of the signal.

The selection of the appropriate window size and order achieves a trade-off between noise reduction and avoiding the introduction of bias. Indeed, the wider the window